PAPER Special Issue on Super Chip for Intelligent Integrated Systems

Graceful Degradation for Multiprocessor Realization of Maximally Flat FIR Digital Filters

Saed SAMADI†, Akinori NISHIHARA† and Nobuo FUJII†, Members

SUMMARY In this paper we propose a method for increasing the reliability in multiprocessor realization of lowpass and highpass FIR digital filters possessing a maximally flat magnitude response. This method is based on the use of array realization of the filter which has been proposed earlier by the authors. It is shown that if a processing module of the array functions erroneously, it is possible to exclude the module and still obtain a lowpass FIR filter. However, as a price we should tolerate a slight degradation in the magnitude response of the filter that is equivalent to a wider transition band. We also analyze the behavior of the filter when our proposed schemes are implemented on more than one module. The justification of our approach is based on that a slight degradation of the spectral characteristics of a filter may be well tolerated in most filtering applications and thus a graceful degradation in the frequency domain can sufficiently reduce the vulnerability to errors.

key words: *graceful degradation, FIR digital filters, modular array realization, digital signal processing*

1. Introduction

"High speed" and "high reliability" are two preeminent key words characterizing today's VLSI technology. Significant developments in electronics industry has made it possible to integrate complex systems into one IC chip in a reliable manner and obtain greater processing speeds. But in highly integrated circuits it is becoming more and more difficult to achieve high reliability. The reliability of a dense and complex IC is not only important at its actual run time but also determines the yield of its fabrication process. Attempts have been made by numerous researchers to boost the reliability of VLSI systems through improving semiconductor processing technologies, introducing fault tolerance into the systems or combining the both techniques [1]. In view of these points, design of special-purpose hardware for high-speed VLSI processing with an augmented reliability has emerged as a challenge. Some approaches to this issue have shown that the schemes for increasing the speed may even result in structures suitable for embedding fault tolerance features [2].

Specifically, in digital signal processing, real time implementation of complicated algorithms has become possible due to the above advancements. Special-purpose VLSI chips are promising for on-line and efficient implementation of signal processing algorithms [3]. Recently, we proposed a specific structure for linear phase, finite impulse response (FIR) digital filters [4] possessing a frequency response of maximally flat (MAXFLAT) type [5]. This structure is a modular array of identical modules (processing elements) that is capable of processing signals in a speed dominated by the speed of addition operation when implemented in a fixed point number system in a multiprocessor environment. This was achieved through an approach that helped us remove all multiplier coefficients, or putting it in a different way, expand multipliers "efficiently" as bit-shifters and adders. Beside the suitability for high-speed processing, the structure enjoys the capability of an efficient realization as a special-purpose hardware using VLSI technology due to its modularity and regularity. However, the processing elements form a rectangular array and therefore the number of adders and delays required for the whole structure is of order $\mathcal{O}(N^2)$ where $2N$ designates the order of the filter.

In this paper we try to make use of the "redundancy" embedded into the structure, in terms of adders and delay elements, for a better reliability. We will not pay any additional price for this reliability; the redundancy has already been provided but for a different purpose, i.e., high-speed filtering. Thus, the reliability we seek here is not a strict fault tolerance. It is a feature ensuring us that the circuit will function despite the existence of faulty processing elements but in a degraded manner; a graceful degradation. In a digital filter this means that the magnitude response will not deviate largely from the nominal value and the filter can still operate as a member of the same class of frequency-selective filters. For example, for a lowpass filter, the degraded filter remains lowpass but spectral characteristics such as cutoff frequencies will not meet the specifications any more. In many filtering applications, a slight deviation from the given specifications is not fatal for the system and can be tolerated to some extent as long as some essential features of the filter are preserved.

In our approach, we do not specify the class of errors occurring at the array. Rather, we simply assume that faults cause errors that manifest themselves as numerical errors at the modules' outputs. Thus we seek methods that yield a reasonable degradation after the faulty modules are excluded from the array. To this end, we first need to detect the errors and locate

Manuscript received November 26, 1993.

†The authors are with the Faculty of Engineering, Tokyo Institute of Technology, Tokyo, 152 Japan.

the faulty module(s). If this method is to be used for enhancing the yield of fabrication process, the error detection can be handled easily through inspecting the impulse responses at output nodes of the array. On-line implementation of the method is not as straightforward and further research should be done to develop efficient methods for locating faulty modules utilizing the unique features of the array.

This paper comprises five sections. Section 2 provides a background on the filter structure and includes necessary definitions. Then, schemes for achieving a graceful degradation in the case of occurrence of errors are proposed in Sect. 3. The schemes are analyzed quantitatively in Sect. 4 which also contains illustrative interpretations of the schemes as deterioration of spectral characteristics of the filter. Finally, the paper is concluded in Sect. 5.

2. Preliminaries

2.1 Notations and Definitions

The degrees of flatness of a MAXFLAT filter at $\omega = 0$ and $\omega = \pi$ are denoted by L and K, respectively. The order of the filter then becomes $2N = 2(L + K - 1)$[6]. The filter structure consists of LK regularly interconnected modules organizing a mesh array as shown in Fig. 1 for a lowpass filter [4]. The module located at row i, column j of the array is denoted by $\mathcal{M}_{i,j}$, and receives two input signals: a horizontal input $h_{i,j}(z)$ and a vertical input $v_{i,j}(z)$. In this paper we handle signals in their z transform format.

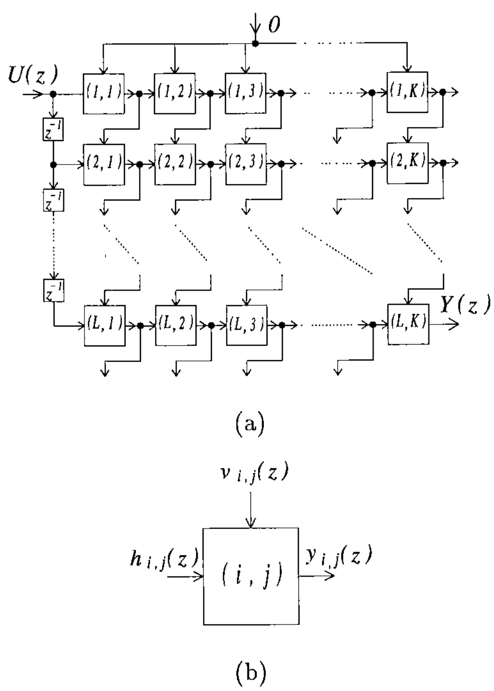

Fig. 1 Rectangular array structure for lowpass MAXFLAT filters. (a) An $L \times K$ array. (b) Input and output signals for $\mathcal{M}_{i,j}$.

The task of $\mathcal{M}_{i,j}$ is processing the input signals and generating an output signal, $y_{i,j}(z)$, that in turn is fed to the neighboring modules at its right and below. The input signal to the filter is denoted by $U(z)$ and the output signal by $Y(z)$. There are two types of boundary signals: horizontal and vertical. By horizontal boundary signals we refer to the signals fed to the array at boundary modules $\mathcal{M}_{i,1}, i = 1(1)L^{\dagger}$, namely $U(z)$ and its delayed versions. Similarly, vertical boundary signals are vertical inputs to boundary modules $\mathcal{M}_{1,j}, j = 1(1)K$, namely 0. To obtain an array for a highpass filter we can simply change the horizontal boundary signals with the vertical ones. The transfer function at the output of $\mathcal{M}_{i,j}$ is denoted by $H_{i,j}(z)$ if all modules $\mathcal{M}_{p,q}$, $p = 1(1)i$, $q = 1(1)j$, generate error-free output signals. The regularity of the structure suggests that $H_{i,j}(z)$ is a MAXFLAT transfer function of degrees of flatness i and j at $\omega = 0$ and $\omega = \pi$, respectively.

By the term "faulty module" we refer to a module that is functioning erroneously due to an arbitrary fault. Whereas a "fault-free module" processes its input signals accurately according to the relationship [4]

$$y_{i,j}(z) = \frac{(1+z^{-1})^2}{4}\, h_{i,j}(z) - \frac{(1-z^{-1})^2}{4}\, v_{i,j}(z). \quad (1)$$

Note that round-off errors occur when implementing the above two-input one-output digital module, and thus an error-free computation can not be performed in its ideal arithmetic meaning. Of course, it is possible to augment the word-length as the signal proceeds through the modules and avoid the round-off errors. But this is not an advisable scheme for a circuit of reasonable cost and complexity. We should, therefore, distinguish the round-off errors, that are inevitable, from any other errors, generated due to faults such as physical defects, that can be avoided. However, this is not generally simple when the filter is actually processing signals. For example, stuck-at errors in the bits of low significance are hard to distinguish from round-off errors.

2.2 Bernstein Representation of Polynomials

An arbitrary polynomial $f(x)$ of degree N can be represented, using Bernstein polynomials, as [7]

$$f(x) = \sum_{i=0}^{N} b_i^{(N)} B_i^{(N)}(x),$$

where

$$B_i^{(N)}(x) = \binom{N}{i} (1-x)^{N-i} x^i,$$

$^{\dagger}i = i_b(i_s)i_e$ is equivalent to $i = i_b, i_b + i_s, i_b + 2i_s, \ldots, i_e$.

are Bernstein basis functions and $b_i^{(N)}$ are called Bernstein coefficients. A shorthand representation for $f(x)$ is

$$f(x) = \{b_0^{(N)}, b_1^{(N)}, \ldots, b_N^{(N)}\}. \tag{2}$$

The magnitude response of the MAXFLAT filter of Fig. 1 can then be written as

$$H_{L,K}(x) = \{\underbrace{1,\ldots,1}_{L}, \underbrace{0,\ldots,0}_{K}\},$$

where

$$x = \left.\frac{1 - \frac{z+z^{-1}}{2}}{2}\right|_{z=\exp(j\omega)}$$

It is possible to represent $f(x)$ in a degree higher than N by recursive application of degree elevation procedure. Through this procedure, the Bernstein representation of $f(x)$ in one degree higher i.e.,

$$f(x) = \{b_0^{(N+1)}, b_1^{(N+1)}, \ldots, b_N^{(N+1)}, b_{N+1}^{(N+1)}\}$$

can be obtained. Note that the corresponding basis functions are $B_i^{(N+1)}(x)$ now. The relationship between $b_i^{(N+1)}$ and $b_i^{(N)}$ becomes [8]

$$b_i^{(N+1)} = \frac{i}{N+1} b_{i-1}^{(N)} + (1 - \frac{i}{N+1}) b_i^{(N)} \tag{3}$$
$$\text{for} \quad i = 0(1)(N+1).$$

From this procedure, it can be understood that unlike the power or monomial representation one can not verify the real (canonical) degree of a polynomial by simple inspection of its Bernstein coefficients. We will use Eq. (3) later for subtracting Bernstein

3. Degradation Schemes

The schemes we propose here result from two simple observations: (1) convergence of Bernstein approximation is slow [9] and (2) MAXFLAT filters are in fact Bernstein approximations of ideal filters [6]. It has been already stated that the transfer function at the output of module $\mathcal{M}_{i,j}$, i.e., $H_{i,j}(z)$, corresponds to a MAXFLAT filter with degrees of flatness i and j. However, the magnitude response of this transfer function does not differ much from that of $H_{i,j-1}(z)$ or $H_{i-1,j}(z)$. Consequently, output signals of neighboring modules resemble each other throughout the array, and if a certain module generates erroneous output signals, we may use an output from a neighboring module instead. In this case the filter will continue to function as a linear phase, FIR system in a degraded manner from the frequency-selectivity point of view, as long as this substitution does not produce a feedback loop.

Let us assume that a fault has occurred at $\mathcal{M}_{i,j}$. The erroneous signal due to this fault, $y_{i,j}(z)$, affects $\mathcal{M}_{i,j+1}$ through $h_{i,j+1}(z)$ and $\mathcal{M}_{i+1,j}$ through $v_{i+1,j}(z)$. In this paper, we devise schemes for substituting these signals with appropriate alternatives from $\mathcal{M}_{i,j-1}$ or $\mathcal{M}_{i-1,j}$. The question is whether the resulting degradation is acceptable for practical applications. To answer this question we should compute the magnitude response of the filter after implementing the schemes. But first, in this section, we give mathematical formulation of the schemes.

3.1 Double Bypass Scheme (DBS)

In this class of schemes which comes to mind as a natural choice, the input signals to the faulty module bypass it to avoid its effect. First, the faulty module $\mathcal{M}_{i,j}$ is excluded by disconnecting its output signal from $\mathcal{M}_{i,j+1}$ and $\mathcal{M}_{i+1,j}$. Then, $\mathcal{M}_{i-1,j}$ and $\mathcal{M}_{i,j-1}$ are connected to $\mathcal{M}_{i+1,j}$ and $\mathcal{M}_{i,j+1}$, respectively, as shown in Fig. 2 (a). This can be expressed as

$$h_{i,j+1}(z) = h_{i,j}(z), \qquad v_{i+1,j}(z) = v_{i,j}(z), \tag{4}$$

equivalently. If the faulty module is a boundary module, appropriate boundary signals can be used by defining

$$h_{0,j}(z) = z^{-(j-1)}U(z), \quad v_{i,0}(z) = 0.$$

3.2 Other Schemes

Figures 2(b), (c) and (d) illustrate other schemes belonging to the same family as the DBS. The members of this family use the outputs of $\mathcal{M}_{i,j-1}$, $\mathcal{M}_{i-1,j}$ or both of them and differ in the degree of degradation they cause and their suitability for implementation in a certain environment. In the rest of this paper we will give detailed computations only for the DBS.

4. Evaluation of Degradation in Frequency Domain

In the following, we will evaluate the proposed schemes by investigating the degradation of the magnitude response of the filter. Although in all cases the eliminated module does not affect the signal flow any more, direct computation of the transfer function of the degraded filter is not straightforward; specially when more than one faultymodule exist. Here we, first, derive a formula for the degraded magnitude response when only one faulty module exists. Then, the mechanism of degradation will be analyzed qualitatively for a general case where an arbitrary number of modules can be faulty. Our idea is utilizing the principal of superposition in the linear signal flow graph of the filter.

4.1 Degradation of Magnitude Response for One Faulty Module

Assume that $\mathcal{M}_{i,j}$ is the faulty module. The filter, after implementing a degradation scheme, is equivalent to a fault-free filter with two additional signal sources of

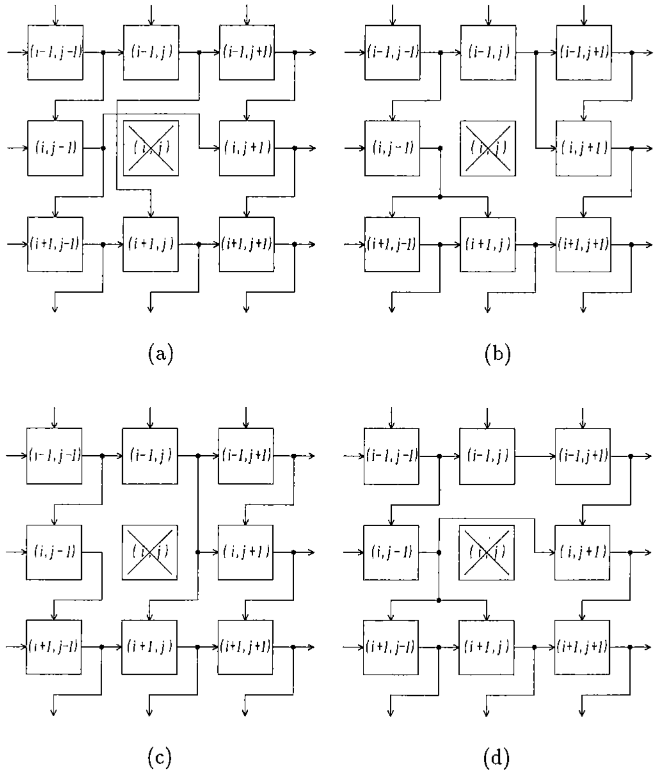

Fig. 2 Graphical illustration of graceful degradation schemes.

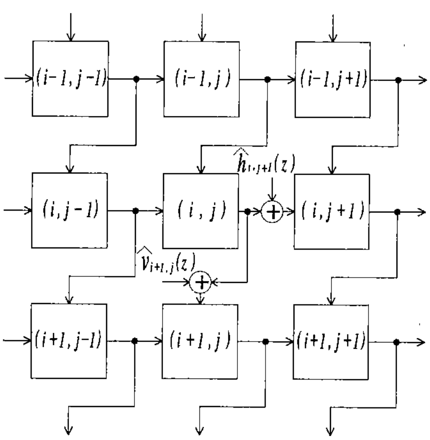

Fig. 3 Equivalent circuit for Fig. 2.

appropriate types at the inputs of $\mathcal{M}_{i,j+1}$ and $\mathcal{M}_{i+1,j}$ as shown in Fig. 3. Specifically, for the DBS we have

$$\begin{aligned}\hat{h}_{i,j+1}(z) &= h_{i,j}(z) - h_{i,j+1}(z) \\ &= y_{i,j-1}(z) - y_{i,j}(z) \\ &= U(z)\left(H_{i,j-1}(z) - H_{i,j}(z)\right), \\ \hat{v}_{i+1,j}(z) &= v_{i,j}(z) - v_{i+1,j}(z) \\ &= y_{i-1,j}(z) - y_{i,j}(z) \\ &= U(z)\left(H_{i-1,j}(z) - H_{i,j}(z)\right).\end{aligned}$$

Hence, the filter would produce an output due to three sources: the boundary signals, $\hat{h}_{i,j+1}(z)$ and $\hat{v}_{i+1,j}(z)$. It can be shown that the magnitude response at the output of the filter of Fig. 1 due to these sources becomes

$$DBS_{i,j}(x) = \{\underbrace{1,\ldots,1}_{L-1}, 1+e_1, e_0, \underbrace{0,\ldots,0}_{K-1}\}, \tag{5}$$

where

$$e_1 = \frac{-\binom{i+j-2}{i-1}\binom{L+K-(i+j+1)}{L-(i+1)}}{\binom{L+K-1}{L-1}},$$

$$e_0 = \frac{\binom{i+j-2}{i-1}\binom{L+K-(i+j+1)}{L-i}}{\binom{L+K-1}{L}}.$$

For a highpass filter we have

$$DBS_{i,j}(x) = \{\underbrace{0,\ldots,0}_{L-1}, -e_1, 1-e_0, \underbrace{1,\ldots,1}_{K-1}\}. \tag{6}$$

For detailed computations see Appendix A.

Let us see what has happened to the magnitude response of the filter. In the Bernstein representation of a magnitude response, it is the number of Bernstein coefficients equal to 1 and 0 that determines the degrees of flatness at $\omega = 0$ and $\omega = \pi$, respectively. Therefore, the flatness of the resulting filters can be determined by inspecting Eq. (5). Three cases can be distinguished.

- $i = L$.
  $e_1 = 0$ and $e_0 \neq 0$; one degree of flatness will be lost at $\omega = \pi$.
- $j = K$.
  $e_1 \neq 0$ and $e_0 = 0$; one degree of flatness will be lost at $\omega = 0$.
- $i \neq L, j \neq K$.
  $e_0 \neq 0$ and $e_1 \neq 0$; one degree of flatness will be lost at both endpoints i.e., $\omega = 0$ and π.

This reveals that the degrees of flatness decrease by, *at most,* one at $\omega = 0$ and $\omega = \pi$ compared to the fault-free filter. Furthermore, $|e_0|, |e_1| \leq 1$ and thus it follows that the magnitude response lies within the interval $[0, 1]$ (see Appendix A).

Same computations can be done for other schemes of Fig. 2. The results are shown in Table 1 which contains the values of e_0 and e_1. It can be seen that in the schemes of Figs. 2 (a) and (b), the effect of degradation is shared between the two endpoints, while the schemes of Figs. 2 (c) and (d) concentrate the degradation at only one of the endpoints.

The spectral interpretation of the degradation is that the schemes cause cutoff frequencies to shift towards filter's passband and stopband or, equivalently, the transition band-width to widen. This is demonstrated in an example for a lowpass filter of order 50 with $L = 9$ and $K = 17$. The effect of the DBS on the magnitude response of the filter is shown in Figs. 4 (a) and (b), where the passband and stopband edge frequencies are plotted versus the location of the faulty module. The passband-edge frequency is defined as the frequency ω_p where $H(x) = 0.95$ and the stopband-edge frequency as the frequency ω_s where $H(x) = 0.05$. For the fault-free filter, ω_p and ω_s are 0.933227 and 1.578079, respectively. For a more visual description of the degradation caused by the scheme, the magnitude responses of the filter, before and after implementing the DBS on $\mathcal{M}_{8,17}$, are shown in Fig. 5.

For the purpose of comparison, we also computed the intervals in which ω_p and ω_s get distributed after implementing the schemes of Fig. 2 on the filter. The results are listed in Table 2 and depicted in Fig. 6 schematically. It can be seen that the schemes of Figs. 2 (a) and (b) behave in the same way and deteriorate both the passband and the stopband. Whereas schemes 2(c) and

Table 1 Values of e_1 and e_0 for the schemes of Fig. 2.

	e_1	e_0
(a)	$-\frac{\binom{i+j-2}{i-1}\binom{L+K-(i+j+1)}{L-(i+1)}}{\binom{L+K-1}{L-1}}$	$\frac{\binom{i+j-2}{i-1}\binom{L+K-(i+j+1)}{L-i}}{\binom{L+K-1}{L}}$
(b)	$-\frac{\binom{i+j-2}{i-1}\binom{L+K-(i+j+1)}{L-i}}{\binom{L+K-1}{L-1}}$	$\frac{\binom{i+j-2}{i-1}\binom{L+K-(i+j+1)}{L-(i+1)}}{\binom{L+K-1}{L}}$
(c)	$-\frac{\binom{i+j-2}{i-1}\binom{L+K-(i+j)}{L-i}}{\binom{L+K-1}{L-1}}$	0
(d)	0	$\frac{\binom{i+j-2}{i-1}\binom{L+K-(i+j)}{L-i}}{\binom{L+K-1}{L}}$

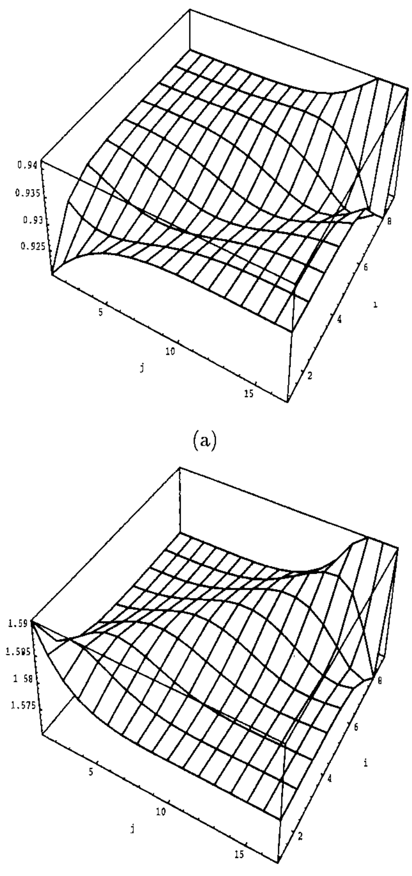
(a)
(b)

Fig. 4 Spectral effects of the DBS. (a) Passband-edge frequency (nominal value: 0.933227) versus the location of faulty module. (b) Stopband-edge frequency (nominal value: 1.578079) versus the location of faulty module.

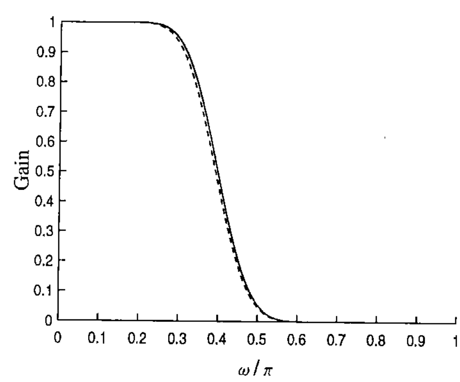

Fig. 5 Gain of the fault-free filter (solid line), and the degraded filter (dashed line) after implementing the DBS on $\mathcal{M}_{8,17}$ versus frequency ω.

Table 2 Intervals of distribution for ω_p and ω_s.

	ω_p	ω_s
(a)	[0.908841, 0.955906]	[1.56388, 1.61366]
(b)	[0.870978, 0.940202]	[1.52824, 1.59096]
(c)	[0.870978, 0.933226]	[1.52824, 1.57808]
(d)	[0.933227, 0.955906]	[1.57808, 1.61366]

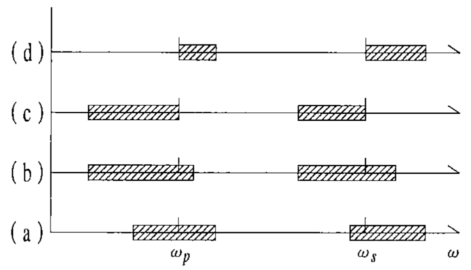

Fig. 6 Schematic depiction of Table 2.

(d) affect only the passband and the stopband, respectively.

4.2 Degradation of Magnitude Response for Multiple Faulty Modules

An exact formula for the magnitude response when more than one faulty module exist would be very difficult to express and derive in general. Hence, we prefer to analyze, qualitatively, the effect of multiple implementation of the schemes on the degrees of flatness. In other words, we are interested in obtaining a rule that tells us how many degrees of flatness will be lost after implementing say, the DBS on d different modules. The following theorem provides us with a simple answer.

Theorem 1: In an array with d faulty modules bypassed using the DBS, the transfer function at the output loses at most d degrees of flatness at each endpoint i.e., $\omega = 0$ and $\omega = \pi$.

See Appendix B for a proof. Similar theorems can be proved for other degradation schemes.

It should be noted that the above theorem is a prediction for the worst possible case. Even in the multiple faulty module case, depending on the locations and number of the faulty modules, the filter may behave like the single faulty module case. That is, only one degree of flatness may decrease at each endpoint. For example in a 4×4 array, with modules $\mathcal{M}_{1,3}$ and $\mathcal{M}_{3,2}$ undergone the DBS, the resulting degrees of flatness are 3 and 3.

5. Conclusions

We showed that the increased redundancy in the array realization of MAXFLAT FIR filters initially proposed as a solution for high-speed signal processing on special-purpose hardware can be used for another important purpose: increasing the reliability. Schemes were proposed for achieving graceful degradation of the magnitude response when a processing module of the array functions erroneously. The schemes were based on the use of the outputs from the nearest modules to the faulty module. This was resulted from simple observations on the mathematical interpretation of the array. It was shown that exclusion of one faulty module from a fault-free array results in the reduction of at most one degree of flatness in the passband and the stopband. However, this causes passband and stopband edge frequencies to deviate from their nominal values. We illustrated this phenomenon in an example where the edge frequencies were calculated for the proposed schemes. The results showed that the schemes behave in different ways; some divided the deterioration "fairly" between the passband and the stopband while some acted in a biased manner towards only one of the them.

To investigate the possibility of multiple implementation of the schemes on an array with more than one faulty module we derived a simple rule that let us predict quantitatively the worst spectral deterioration. Specifically, it was shown that implementing the DBS, d times on the array would result in the reduction of at most d degrees of flatness at the two endpoints. Although this is not sufficient for predicting the exact shape of the magnitude response, it can be expected that the filter remains in the same category of frequency-selective filters if $d < \min\{L, K\}$.

Off-line use of the schemes is suitable for enhancing the yield in the production line where the location of the faulty module can be detected through measuring the impulse responses at the output nodes of the array and comparing them with their expected values. In this case, the roundoff errors can be taken into account when computing the expected values and thus their effect can be distinguished from other errors. However, developing an efficient method for on-line location of the faulty module(s) remains an open problem.

A significant feature of our approach is that we have merely utilized the increased redundancy imposed on the filter structure for the purpose of efficient realization and high-speed processing.

References

[1] See for example, *Proc. IEEE*, Special Issue on VLSI reliability, May 1993.
[2] Jou, J.Y. and Abraham, J.A., "Fault-tolerant matrix arithmetic and signal processing on highly concurrent computing structures," *Proc. IEEE*, vol.74, no.5, pp.732–741, May 1986.
[3] Kung, S.Y., *VLSI array processing*, Prentice Hall, 1988.
[4] Samadi, S., Cooklev, T., Nishihara, A., and Fujii, N., "Multiplierless structure for maximally flat linear phase FIR digital filters," *Electron. Lett.*, vol.29, no.2, pp.184–185, 1993.
[5] Herrmann, O., "On the approximation problem in nonrecursive digital filter design," *IEEE Trans. Circuit Theory*, vol.CT-18, pp.411–413, 1971.

[6] Rajagopall, L.R. and Dutta Roy, S.C., "Design of maximally-flat FIR filters using the Bernstein polynomial," *IEEE Trans. Circuits Systs.*, vol.CAS-34, no.12, pp.1587–1590, 1987.
[7] Cargo, G.T. and Shisha, O., "The Bernstein form of a polynomial," *Journal of Research of the National Bureau of Standards-B.*, vol.70B, no.1, pp.79–81, 1966.
[8] Farouki, I.T. and Rajan, V.T., "Algorithms for polynomials in Bernstein from," *Computer Aided Geometric Design*, vol.5, pp.1–26, 1988.
[9] Davis, P. J., *Interpolation and approximation,* Dover Publications, Inc., New York, 1975.

Appendix A: Derivation of Eq. (5)

The transfer function of the array of Fig. 2 after implementing the DBS becomes

$$\begin{aligned} &DBS_{i,j}(z) \\ &= H_{L,K}(z) + \\ &\{H_{i,j-1}(z) - H_{i,j}(z)\}\, H_{(i,j+1)\to(L,K)}(z) \\ &+ \{H_{i-1,j}(z) - H_{i,j}(z)\}\, H_{(i+1,j)\to(L,K)}(z), \end{aligned}$$

where $H_{(i,j+1)\to(L,K)}(z)$ and $H_{(i+1,j)\to(L,K)}(z)$ denote the transfer functions from the horizontal input of $\mathcal{M}_{i,j+1}$ and the vertical input of $\mathcal{M}_{i+1,j}$ to the filter output respectively. In terms of magnitude response, we may write

$$\begin{aligned} &DBS_{i,j}(x) \\ &= \sum_{p=0}^{L-1} B_p^{(L+K-1)}(x) \\ &+ \underbrace{\left(\sum_{p=0}^{i-1} B_p^{(i+j-2)}(x) - \sum_{p=0}^{i-1} B_p^{(i+j-1)}(x)\right) \binom{L-i+K-(j+1)}{L-i} (1-x)^{K-j} x^{L-i}}_{H_{(i,j+1)\to(L,K)}(x)} \\ &+ \underbrace{\left(\sum_{p=0}^{i-2} B_p^{(i+j-2)}(x) - \sum_{p=0}^{i-1} B_p^{(i+j-1)}(x)\right) \binom{L-(i+1)+K-j}{L-(i+1)} (1-x)^{K-j} x^{L-i}}_{H_{(i+1,j)\to(L,K)}(x)}. \end{aligned}$$

To subtract the Bernstein representations of different degrees we use the degree elevation procedure (3) and obtain

$$\begin{aligned} &DBS_{i,j}(x) \\ &= \sum_{p=0}^{L-1} B_p^{(L+K-1)}(x) \\ &+ \frac{i}{i+j-1} \binom{i+j-1}{i} (1-x)^{j-1} x^{i} \\ &\binom{L-i+K-(j+1)}{L-i} (1-x)^{K-j} x^{L-i} \\ &+ \frac{-j}{i+j-1} \binom{i+j-1}{i-1} (1-x)^{j} x^{i-1} \\ &\binom{L-i+K-(j+1)}{L-(i+1)} (1-x)^{K-j} x^{L-i}, \end{aligned}$$

or

$$\begin{aligned} DBS_{i,j}(x) &= \sum_{p=0}^{L-1} B_p^{L+K-1}(x) \\ &+ e_1\, B_{L-1}^{(L+K-1)}(x) + e_0\, B_L^{(L+K-1)}(x). \end{aligned}$$

For the highpass case, we can simply subtract the above function from 1.

It is also important to show

$$|e_0| < 1 \quad \text{and} \quad |e_1| < 1$$

to prove that the magnitude response lies within $[0, 1]$. Here we show this for e_0. From the identity

$$\sum_{r=0}^{p} \binom{n}{r} \binom{m}{p-r} = \binom{n+m}{p} \quad \text{for} \quad p \leqq n+m,$$

we have

$$\binom{n}{r} \binom{m}{p-r} \leqq \binom{n+m}{p} \quad \text{for} \quad 0 \leqq r \leqq p \quad \text{and} \quad p \leqq n+m.$$

Now let

$$\begin{aligned} n &= i+j-2, & r &= i-1, \\ m &= L+K-i-j-1, & p &= L-1. \end{aligned}$$

Obviously, these values are valid to be used in the inequality if the following conditions hold:

$$\begin{aligned} &p \leqq n+m \quad \Rightarrow \quad K \geqq 2 \\ &r \leqq p \quad \Rightarrow i \leqq L. \end{aligned}$$

The only condition that may not always hold is $K \geqq 2$. However, it can be easily seen that if $K = 1$, $e_0 = \frac{1}{L}$ and the theorem holds for this case. Hence we can write

$$\binom{i+j-2}{i-1} \binom{L+K-i-j-1}{L-i} \leqq \binom{L+K-3}{L-1}.$$

Thus we have

$$|e_0| \leqq \frac{\binom{L+K-3}{L-1}}{\binom{L+K-1}{L}} < 1.$$

The same inequality can be used to prove $|e_1| < 1$.

Appendix B: Proof of Theorem 1

Proof: The theorem can be proved by induction on d but, first, we need to define the concept of "DBS-affected modules." We say that a module is DBS-affected of order d if and only if

- there are d faulty modules in the array undergone the DBS and,
- there is a faulty module of order $(d-1)$ such that the both input signals to the module of our concern are affected by it.

To complete this definition we define the zeroth order DBS-affected module as a module that neither of its input signals are affected by faulty module(s) existing in the array (cf. Fig. A·1).

- $d = 1$.
  The correctness of the theorem for this case is obvious from Sect. 4.1.
- $d = d$.
  We assume that the theorem holds for this case and proceed to the next part.
- $d = d + 1$.
  We have totally $(d+1)$ faulty modules. Now we pick a DBS-affected faulty module with maximum order, which we denote by $\mathcal{M}_{i,j}$. Since this theorem deals with the maximum possible number of lost degrees of flatness, we assume that $\mathcal{M}_{i,j}$ is of order d; the worst case. Based on this assumption the magnitude responses at the two horizontal and vertical inputs of this module, i.e., $\hat{H}_{i,j-1}(x)$ and $\hat{H}_{i-1,j}(x)$ can be written as

$$\hat{H}_{i,j-1}(x) = \{\underbrace{1,\ldots,1}_{i-d},\underbrace{\star,\ldots,\star}_{2d},\underbrace{0,\ldots,0}_{j-d-1}\},$$
$$\hat{H}_{i-1,j}(x) = \{\underbrace{1,\ldots,1}_{i-d-1},\underbrace{\star,\ldots,\star}_{2d},\underbrace{0,\ldots,0}_{j-d}\},$$

where $\star$ represents a real number. Now, we use the principle of superposition in the same way as Appendix A, but will represent functions in their shorthand Bernstein format for sake of simplicity. here, unlike Appendix A, we do not want to obtain a precise formula for the magnitude response and suffice it to count the number of 0's and 1's of the Bernstein coefficients. Using the degree elevation procedure (3), we have

$$\begin{aligned}
&\left(\hat{H}_{i,j-1}(x) - \hat{H}_{i,j}(x)\right) H_{(i,j+1)\to(L,K)}(x) \\
&= \{\underbrace{0,\ldots,0}_{i-d},\underbrace{\star,\ldots,\star}_{2d+1},\underbrace{0,\ldots,0}_{j-d-1}\} \\
&\binom{L-i+K-(j+1)}{L-i}(1-x)^{K-j}x^{L-i} \\
&= \{\underbrace{0,\ldots,0}_{L-d},\underbrace{\star,\ldots,\star}_{2d+1},\underbrace{0,\ldots,0}_{K-d-1}\}.
\end{aligned}$$

Similarly,

$$\begin{aligned}
&\left(\hat{H}_{i-1,j}(x) - \hat{H}_{i,j}(x)\right) H_{(i+1,j)\to(L,K)}(x) \\
&= \{\underbrace{0,\ldots,0}_{L-d-1},\underbrace{\star,\ldots,\star}_{2d+1},\underbrace{0,\ldots,0}_{K-d}\}.
\end{aligned}$$

Thus the magnitude response becomes

$$\begin{aligned}
&\{\underbrace{1,\ldots,1}_{L},\underbrace{0,\ldots,0}_{K}\} \\
&+ \{\underbrace{0,\ldots,0}_{L-d},\underbrace{\star,\ldots,\star}_{2d+1},\underbrace{0,\ldots,0}_{K-d-1}\} \\
&+ \{\underbrace{0,\ldots,0}_{L-d-1},\underbrace{\star,\ldots,\star}_{2d+1},\underbrace{0,\ldots,0}_{K-d}\} \\
&= \{\underbrace{1,\ldots,1}_{L-d-1},\underbrace{\star,\ldots,\star}_{2d+2},\underbrace{0,\ldots,0}_{K-d-1}\}. \qquad \square
\end{aligned}$$

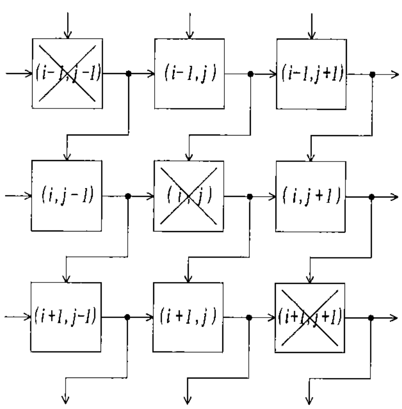

(a)

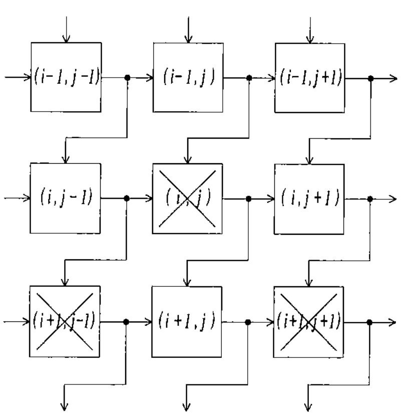

(b)

Fig. A·1 An example of DBS-affected modules. (a) $\mathcal{M}_{i+1,j+1}$ is of order 2. (b) $\mathcal{M}_{i+1,j+1}$ is of order 1.

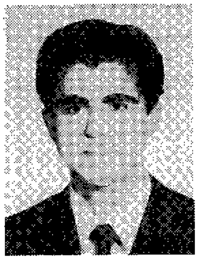

Saed Samadi was born in Tehran, Iran in 1966. He received the B.E. and M.E. degrees in Physical Electronics from Tokyo Institute of Technology in 1989 and 1991, respectively. He is currently a doctoral student in the department of Physical Electronics at Tokyo Institute of Technology. His research interests are in Digital Signal Processing.

Akinori Nishihara was born in Fukuoka, Japan on February 26, 1951. He received the B.E., M.E. and Dr. Eng. degrees in electronics from Tokyo Institute of Technology in 1973, 1975 and 1978, respectively. Since 1978 he has been with Tokyo Institute of Technology, where he is now Associate Professor of Department of Physical Electronics, Faculty of Engineering. His main research interests are in filter design, 1D and multi-D signal processing, and modern applications of classical circuit theory. Since 1990 he has been serving as an Associate Editor of the IEICE Trans. Fundamentals. Dr. Nishihara is a member of IEEE, EURASIP and ECS.

Nobuo Fujii received a B.E. degree from Keio University, Yokohama, Japan, and M.E. and Doctor of Engineering degrees from Tokyo Institute of Technology, Tokyo, Japan, in 1966, 1968, and 1971, respectively. Since 1971, he has been with the Faculty of Engineering, Tokyo Institute of Technology where he is now a professor in the department of Physical Electronics. From 1984 to 1985, he was a visiting scholar at the University of California, Santa Barbara. His main interest lies in the field of active network theory and analog integrated circuits. He is the recipient of the 1983 Best Paper Award of the Institution of Electrical and Communication Engineers of Japan. He is the author of 5 books. Dr. Fujii is a member of the Institution of Electrical and Electronics Engineers, and the Institution of Electrical Engineers of Japan.